SPAWAR
Systems Center
PACIFIC

TECHNICAL REPORT 3030
September 2016

Preliminary Work in Atmospheric Turbulence Profiles with the Differential Multi-image Motion Monitor

Kristopher. B. Gibson

SSC Pacific
San Diego, CA 92152-5001

SSC Pacific
San Diego, California 92152-5001

K. J. Rothenhaus, CAPT, USN
Commanding Officer

C. A. Keeney
Executive Director

ADMINISTRATIVE INFORMATION

The work described in this report was performed by the Littoral Engineering Branch (Code 56430) of the Maritime Systems Division (Code 56400), Space and Naval Warfare Systems Center Pacific (SSC Pacific), San Diego, CA. The Optical Channel Characterization in Maritime Atmospheres (OCCIMA) project was funded by the Naval Innovative Science and Engineering (NISE) Program at SSC Pacific under the NISE Capability Investment category.

Released by
B. Clulow, Head
Littoral Engineering Branch

Under authority of
M. H. Berry, Head
Maritime Systems Division

SB

EXECUTIVE SUMMARY

This report provides the background to anisoplanatic jitter and how that relates to Zernike tilt covariance and ultimately the C_n^2 path profile. Space and Naval Warfare Systems Center Pacific's (SSC Pacific) Optical Channel Characterization in Maritime Atmospheres (OCCIMA) Python code is demonstrated with examples that match prior work from past experiments with anisoplanatic jitter. A new experiment using a dual imaging system instead of a single imaging system is presented. And finally, this report demonstrates how to estimate the C_n^2 profile given jitter measurements.

CONTENTS

Figures

Tables

1. INTRODUCTION

In my previous work [1], I proposed a modified differential image motion monitor (DIMM), the Differential Multi-image Motion Monitor (DM3), by using a stereo imaging apparatus. With this approach, the theory for estimating an averaged path C_n^2 was possible. Additionally, the image pairs were aligned for a more effective turbulence mitigation algorithm. There exists work related to this effort by Whiteley [2]. In their approach, features are also tracked as in my method but the C_n^2 path profile is estimated instead of the average path. This is a much better approach to atmospheric turbulence estimation because more information is gained from the scene.

In this paper, I will first provide the background in tilt anisoplanatism, demonstrate an example using the present version of Space and Naval Warfare Systems Center Pacific's Optical Channel Characterization in Maritime Atmospheres (OCCIMA) Python code, show how to model the DM3 and anisoplanitic jitter measurements, and finally demonstrate how the turbulence strength profile can be estimated with any imaging configuration given jitter measurements.

2. BACKGROUND

2.1 INDEX-OF-REFRACTION STRUCTURE CONSTANT C_N^2

There is a rich set of literature discussing the parameters of atmospheric turbulence for which I refer the reader [3–7]. In short, the strength of the turbulence may be expressed with an atmospheric index-of-refraction structure constant, C_n^2. This constant is proportional to the variation of index-of-refraction differences within the atmosphere along the imaging path.

The assumption that C_n^2 is homogeneous along an imaging path is not a reasonable assumption because of random wind velocities, heat sources, etc. Instead, a function of the path distance, z, is used to characterize C_n^2 as a varying parameter: $C_n^2 \rightarrow C_n^2(z)$.

Many methods exist that estimate parameters that are *path averages* of $C_n^2(z)$, which is an integration along the path. These methods estimate different atmospheric parameters that are related to a weighted path average of $C_n^2(z)$ [2]:

$$\text{Fried parameter: } r_0 = \left(\frac{2.91}{6.88} \left(\frac{2\pi}{\lambda} \right)^2 L \int_0^1 d\xi C_n^2(\xi L)(1-\xi)^{5/3} \right)^{-3/5} \tag{1}$$

$$\text{isoplanatic angle: } \theta_0 = \left(2.91 \left(\frac{2\pi}{\lambda} \right)^2 L^{8/3} \int_0^1 d\xi C_n^2(\xi L)\xi^{5/3} \right)^{-3/5} \tag{2}$$

$$\text{integrated turbulence: } m_0 = \int_0^1 d\xi C_n^2(\xi L) \tag{3}$$

$$\text{Rytov parameter: } \sigma_\chi^2 = 0.5631 \left(\frac{2\pi}{\lambda} \right)^{7/6} L^{11/6} \int_0^1 d\xi C_n^2(\xi L)[\xi(1-\xi)]^{5/6}. \tag{4}$$

Therefore if the C_n^2 profile can be estimated, then the above turbulence parameters can then be estimated.

2.2 ZERNIKE CIRCLE POLYNOMIALS

When imaging through a turbulent atmosphere, the wavefront arriving at the sensor (or sensors) is distorted. One way to model this wavefront distortion is using the Zernike circle polynomials with Noll's convention [8]. Since most of the warping is in the tilt modes [6], I show only the first three Zernike polynomials in Table 1. The wavefront (in circular coordinates) can then be represented by the Zernike coefficients a_i:

$$\phi(r,\theta) = \sum_{i=1}^{\infty} a_i Z_i(r,\theta). \tag{5}$$

Analogous to signal decomposition, the wavefront can be decomposed into Zernike coefficients:

$$a_i = \frac{\int_0^{2\pi} \int_0^1 W(r,\theta) Z_i(r,\theta) r dr d\theta}{\int_0^{2\pi} \int_0^1 Z_i^2(r,\theta) r dr d\theta}. \tag{6}$$

The Zernike tilt modes, a_i, can be related to the measured angular tilt measurement θ (units of λ/D) with $a = \frac{2}{\pi}\theta$, where λ is the wavelength and D is the aperture diameter [2].

Table 1. First three Zernike polynomials.

n	m	i	$\mathbf{Z_n^m(r,\theta)}$	Name
0	0	1	1	piston
1	1	2	$2r\cos\theta$	x tilt
1	1	3	$2r\sin\theta$	y tilt

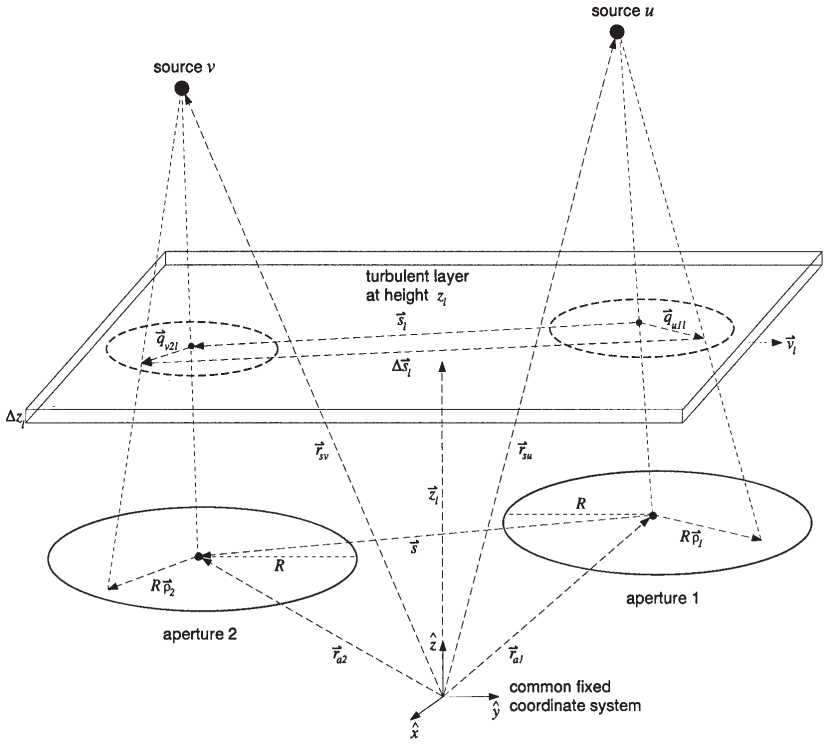

Figure 1. Illustration of a general dual aperture configuration with pairs of sources from Whiteley [9].

2.3 DUAL APERTURE CONFIGURATION

The general dual aperture geometry as portrayed by Whiteley is illustrated in Figure 1. In this configuration, there are two sources, u and v, that are observed by apertures 1 and 2, respectively. Their respective phases can be modeled with Zernike polynomials

$$\phi_{u1}(R\vec{\rho}_1) = \sum_{i=1}^{\infty} a_{u1i} Z_i(\vec{\rho}_1), \tag{7}$$

$$\phi_{v2}(R\vec{\rho}_2) = \sum_{j=1}^{\infty} a_{v1j} Z_j(\vec{\rho}_2), \tag{8}$$

with phase from source u through aperture 1 and order i as a_{u1i} and source v through aperture 2 and order j. Whiteley calculated the cross-correlation of the Zernike coefficients as

$$\langle a_{u1i} a_{v2j} \rangle = \left(\frac{D_1}{r_0}\right)^{5/3} \sqrt{3}\Gamma(8/3)2^{-5/3}\frac{6.88}{2.91}\left(\frac{D_2}{D_1}\right) F \sum_l w_l[(1-A_{u1l})(1-A_{v2l})]^{-1} \times \begin{cases} G_{i,j}\int_0^\infty \frac{dx}{x}(x^2+x_0^2)^{-11/6} J_{(m_i+m_j)}\left[\frac{2s_l}{D_1}x\right] \\ \quad \times J_{(n_i+1)}\left[(1-A_{u1l})x\right] J_{(n_j+1)}\left[\frac{D_2}{D_1}(1-A_{v2l})x\right] \\ +H_{i,j}\int_0^\infty \frac{dx}{x}(x^2+x_0^2)^{-11/6} J_{|m_i-m_j|}\left[\frac{2s_l}{D_1}x\right] \\ \quad \times J_{(n_i+1)}\left[(1-A_{u1l})x\right] J_{(n_j+1)}\left[\frac{D2}{D1}(1-A_{v2l})x\right] \end{cases}, \tag{9}$$

where

$$F \equiv [(n_i+1)(n_j+1)]^{1/2}(-1)^{\frac{1}{2}(n_i+n_j)}2^{[1-\frac{1}{2}(\delta_{m_i0}+\delta_{m_j0})]}(-1)^{m_j}, \tag{10}$$

$$G_{i,j} \equiv (-1)^{\frac{3}{2}(m_i+m_j)}\cos[(m_i+m_j)\phi_{s_l} + \pi/4\left\{(1-\delta_{m_i0})[(-1)^i-1]+(1-\delta_{m_j0})[(-1)^j-1]\right\}], \tag{11}$$

$$H_{i,j} \equiv (-1)^{\frac{3}{2}|m_i-m_j|}\cos[(m_i-m_j)\phi_{s_l} + \pi/4\left\{(1-\delta_{m_i0})[(-1)^i-1]+(1-\delta_{m_j0})[(-1)^j-1]\right\}], \tag{12}$$

and D_1 and D_2 are the aperture diameters for 1 and 2, respectively. The terms n_i, m_i are Zernike modes and the subscript i (or j) is the "Noll's order" for the different modes. The magnitude of the aperture separation projected onto layer l is s_l. $J_k[\cdot]$ is a Bessel function of order k of the first kind. The angle ϕ_{s_l} is the angle between the coordinate $\hat{x}$ and aperture vector $\vec{s}$. In Equation (9), the assumption is made that the turbulence induced phase is wide-sense stationary and isotropic and that the von Kármán spectrum is valid.

The only interest in this paper is for tilt in the $\hat{x}$ and $\hat{y}$ directions. Therefore the values for $n_i = m_i = 1$ for $i, j = 2$ or 3. Where $i = 2$ is the Noll order for tilt in the $\hat{x}$ direction and $i = 3$ is the Noll order for tilt in the $\hat{y}$ direction. The F, G, H coefficients simplify to

$$F = 4, \tag{13}$$

$$G_{i,j} = -\cos\left[2\phi_{s_l} + \frac{\pi}{4}\left\{[(-1)^i-1]+[(-1)^j-1]\right\}\right], \tag{14}$$

$$H_{i,j} = \cos\left[\frac{\pi}{4}\left\{[(-1)^i-1]+[(-1)^j-1]\right\}\right]. \tag{15}$$

Another assumption is made to make the integrals in Equation (9) more tractable. With $x_0 \equiv \pi D_{1,2}/L_0$ and outer scale L_0 and aperture diameter $D_{1,2}$, Equation (9) can be simplified with an assumption that $D \ll L_0 \implies x_0 \approx 0$,

$$\langle a_{u1i} a_{v2j} \rangle = \left(\frac{D_1}{r_0}\right)^{5/3} \sqrt{3}\Gamma(8/3)2^{1/3}\frac{6.88}{2.91}\left(\frac{D_2}{D_1}\right) \sum_l w_l[(1-A_{u1l})(1-A_{v2l})]^{-1} \times \begin{cases} G_{i,j}\int_0^\infty \frac{dx}{x}x^{-11/3} J_2\left[\frac{2s_l}{D_1}x\right] \\ \quad \times J_2\left[(1-A_{u1l})x\right] J_2\left[\frac{D_2}{D_1}(1-A_{v2l})x\right] \\ +H_{i,j}\int_0^\infty \frac{dx}{x}x^{-11/3} J_0\left[\frac{2s_l}{D_1}x\right] \\ \quad \times J_2\left[(1-A_{u1l})x\right] J_2\left[\frac{D2}{D1}(1-A_{v2l})x\right] \end{cases}, \tag{16}$$

with

$$\Delta z_l C_n^2(z_l) = \frac{6.88}{2.91} w_l r_0^{-5/3}, \tag{17}$$

$$\text{and} \quad \sum_l \Delta z_l C_n^2(z_l) = \int_0^L dz C_n^2(z), \tag{18}$$

the cross-correlation of the Zernike coefficients with relation to $C_n^2(z)$ is

$$\langle a_{u1i} a_{v2j} \rangle = 2^{1/3}\sqrt{3}\Gamma(8/3)\left(\frac{2\pi}{\lambda}\right)^2 D_1^{5/3}\left(\frac{D_2}{D_1}\right)\int_0^L dz C_n^2(z)[(1-A_{u1l})(1-A_{v2l})]^{-1}$$
$$\times \begin{cases} G_{i,j}\int_0^\infty \frac{dx}{x} x^{-11/3} J_2\left[\frac{2s(\xi)}{D_1}x\right] \\ \quad \times J_{(n_i+1)}\left[(1-A_{u1l})x\right] J_2\left[\frac{D_2}{D_1}(1-A_{v2l})x\right] \\ +H_{i,j}\int_0^\infty \frac{dx}{x} x^{-11/3} J_0\left[\frac{2s(\xi)}{D_1}x\right] \\ \quad \times J_2\left[(1-A_{u1l})x\right] J_2\left[\frac{D2}{D1}(1-A_{v2l})x\right] \end{cases}. \tag{19}$$

Up to this point, I haven't described A_{u1l} and A_{v2l}. These are layer scaling factors for sources u and v, respectively. With the apertures on the same $\hat{x}-\hat{y}$ plane, these scaling factors are the ratio of path length to the layer divided by the total path length to the source, z/L, if both sources are L distance from the apertures.

Assuming $D = D_1 = D_2$ and that the apertures are on the same imaging plane with respect to the turblence layer and with a change of variables, $\xi = z_l/L = A_{u1l} = A_{v2l}$, $s_l = s(\xi)$, and $\sigma = 2s(\xi)/D$, and indicating Zernike tilt coefficients with $\theta_{u1i} = a_{u1i}$ for $i = 2,$ or 3, Equation (19) becomes

$$\langle \theta_{u1i} \theta_{v2j} \rangle = 16\sqrt{3}\Gamma(8/3)\left(\frac{2\pi}{\lambda}\right)^2 D^{5/3} L \int_0^1 d\xi C_n^2(L\xi) W_{i,j}(\xi;\sigma), \tag{20}$$

in units of $(\lambda/D)^2$. In units of rad^2, the covariance is

$$\langle \theta_{u1i} \theta_{v2j} \rangle = 2^{10/3}\sqrt{3}\Gamma(8/3) D^{-1/3} L \int_0^L d\xi C_n^2(\xi L) W_{i,j}(\xi;\sigma). \tag{21}$$

The term $W_{i,j}(\xi;\sigma)$ is the weighting function that encapsulates the right-hand-side of Equation (19) and is discussed in detail in the next section.

2.4 WEIGHTING FUNCTION

The closed form representation of the weighting function $W_{i,j}(\xi;\sigma)$ has been presented by Whiteley [2] and most recently Magee, Das, and Welch [10]. This weight function is dependent only on the scene geometry and not on the atmosphere. Thus for each source separation and image (or imaged pair), there exists a weight function. An example of a normalized weight curve is illustrated in Figure 2. In Figure 2, the normalized weight is

$$w(\xi;\sigma) = W(\xi;\sigma) / \int_0^1 W(\xi;\sigma). \tag{22}$$

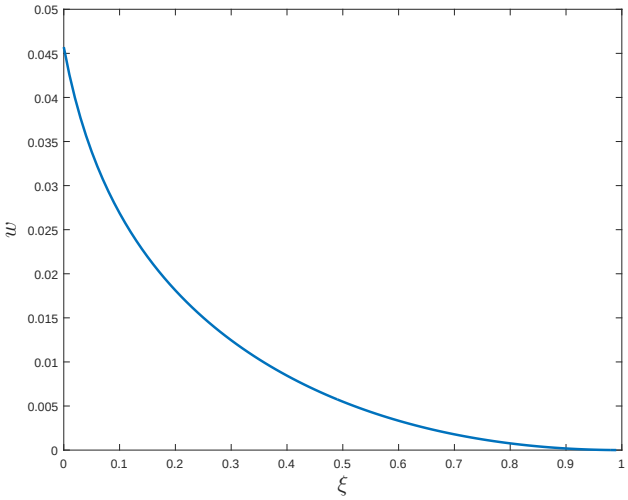

Figure 2. Example of normalized path length (ξ) vs. normalized weight function (w).

3. ANISOPLANATIC JITTER

I will now introduce the relationship between jitter measurements, Zernike coefficient covariance and the main goal of this work, atmospheric turbulence C_n^2 profile. It is best portrayed similar to Magee, Das, and Welch [10] where there are two features and one aperture thus $\theta_i = \theta_{u1i} = \theta_{u2i}$. Here I denote the x-axis as the Zernike tilt order $i = 2$ and y-axis as Zernike tilt order $i = 3$ (θ_x and θ_y respectively). The first and second features' instantaneous angular tilts are

$$\theta(\mathbf{r}) = (\theta_x(\mathbf{r}), \theta_y(\mathbf{r}))^T, \tag{23}$$

$$\theta(\mathbf{r_m}) = (\theta_x(\mathbf{r_m}), \theta_y(\mathbf{r_m}))^T, \tag{24}$$

respectively. The location of the targets are $\mathbf{r}$ and $\mathbf{r_m}$ which are both vectors in three-space $\in \mathbb{R}^3$. The jitter measurements which is the tilt anisoplanatism are related to the correlations of Zernike tilt coefficients with

$$(\sigma_x^2, \sigma_y^2)^T = \text{diag}\left(2\langle\theta(\mathbf{r})\theta^T(\mathbf{r})\rangle - 2\langle\theta(\mathbf{r})\theta^T(\mathbf{r_m})\rangle\right). \tag{25}$$

The relationship between the tilt covariance matrix components (in rad^2) can be related to C_n^2 with

$$\langle\theta_u(\mathbf{r}_i)\theta_v(\mathbf{r}_j)\rangle = 2^{10/3}\sqrt{3}\Gamma(8/3)D^{-1/3}L\int_0^1 d\xi C_n^2(\xi L)W_{uv}(\xi;\sigma). \tag{26}$$

Jitter can be predicted with known C_n^2 and scene geometry by using Equation (26) into Equation (25). This is exactly the case in the work from Magee, Das, and Welch [10].

```
import matplotlib
import numpy as np
import matplotlib.pyplot as plt
import scipy.io as sio
from OCCIMA.atmosphere.atmosgeo import geo, atmos
# Target separations in meters
b = [0, 0.1, 0.2, 0.5, 1, 2, 4, 8]
# Platform altitude in meters
hp = [1550., 1850., 2750., 4250.]
# Target altitude in meters
ht = [1250.]
# Range to target
down_range = 20000.
# Turbulence multiplier
tm = 2.0
# Diameter of platform lens
D = 1.5
wavelength = 1.06e-6
# Number of turbulent screens
number_of_screens = 200
# loading Cn2 screens
magee_data =
sio.loadmat('OCCIMA/testdata/testdata_simulateMagee2003.mat')
jitters_p = np.zeros((len(b), len(hp))).astype(float)
jitters_t = np.zeros((len(b), len(hp))).astype(float)
# Creates most of the atmospheric model
# manipulate the model in the next section
Atm = atmos(slant_range=down_range, ht=ht[0], diameter=[D],
  number_of_screens=number_of_screens, wavelength=wavelength)
```

Listing 1. OCCIMA code example for setting up variables to simulate work by Magee, Das, and Welch [10].

4. OCCIMA CODE EXAMPLE

4.1 COMPARISON WITH MZA ATMTOOLS

Magee, Das, and Welch [10] use their MZA ATMTools software to simulate the anisoplanatic jitter. In their work, they calculate anisoplanatic jitter for different target separations and platform altitudes. They show how jitter changes when these scene geometries change. Similarly, I have OCCIMA software that achieves the same results. In Listing 1, I demonstrate how to setup the scene geometries using OCCIMA modules. The target separations are along the x-axis which is parallel with the x-axis of the imaging system. Therefore, all vertical (y-axis) separation is zero. In Listing 2 each jitter is measured for each platform altitude and target separation. Notice that there are four different weight vectors computed which is in Equation (25). As shown in Figure 3, there is excellent agreement between the OCCIMA code and MZA ATMTools for anisoplanatic jitter simulation in Magee, Das, and Welch [10].

```
for ii in range(0, len(b)):
  for jj in range(0, len(hp)):
    # Set the platform altitude
    Atm.geo.hp = hp[jj]
    # Make sure to re-build the internal values (xi, L, etc.)
    Atm.buildInternalValues()
    # Target [angular separation (radians),
    # orientation w.r.t separation vector]
    # For this example it is horizontal (x-direction)
    target = [b[ii]/Atm.L, 0.0]
    # A single lens is used
    platform = [0.0, 0.0]
    # compute the displacement vector
    d = Atm.computePathDisplacement(platform, target)
    alpha = d / Atm.diameter
    zero_v = np.zeros_like(d)
    # Compute all the weights
    Wpp0 = Atm.computeTiltCovariancePathWeight(zero_v,
        Atm.P_AXIS, Atm.P_AXIS).flatten()
    Wtt0 = Atm.computeTiltCovariancePathWeight(zero_v,
        Atm.T_AXIS, Atm.T_AXIS).flatten()
    Wppm = Atm.computeTiltCovariancePathWeight(alpha,
        Atm.P_AXIS, Atm.P_AXIS).flatten()
    Wttm = Atm.computeTiltCovariancePathWeight(alpha,
        Atm.T_AXIS, Atm.T_AXIS).flatten()
    Atm.Cn2 = magee_data['data']['All_CN2'][0][0][:, index]
    Atm.Cn2 = tm*Atm.Cn2[:].reshape(-1,1)
    # Measure jitter
    jitters_p[ii, jj], jitters_t[ii,jj] =
      Atm.computeAnisoplanaticJitter(Wpp0, Wppm, Wtt0, Wttm)
    index = index + 1
```

Listing 2. Code to generate jitter measurements for each platform altitude and target separation values.

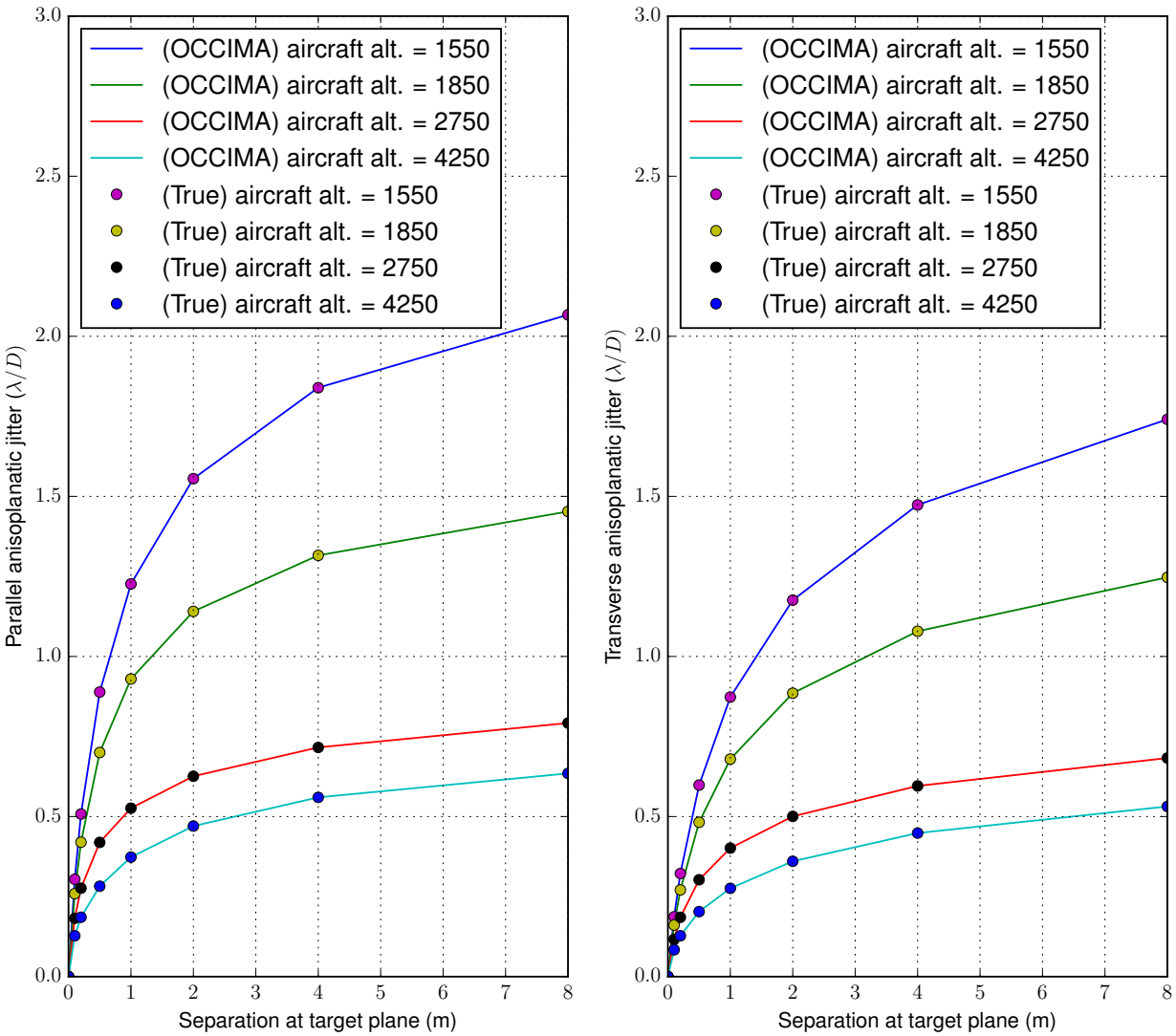

Figure 3. Comparison of OCCIMA software simulation with results from MZA ATMTools (labeled as "True").

4.2 NEW EXPERIMENT WITH DUAL APERTURES

I can do another experiment that is not done in Magee, Das, and Welch [10]. I can choose instead to have dual aperture separations (same diameters) and a source pair separated by 2 meters; hence a multi-imaging motion monitor. The experimental setup is exactly the same except there is a single source separation pair and the previous separations are used instead for the platform separations. The code change is very simple and shown in Listing 3. By changing the separation value σ at each normalized path location ξ, the weight computations are manipulated. The results are plotted in Figure 4.

In Figure 4, it is interesting to note that there is an exponential increase in jitter at lower altitudes as the separation is increased. If the desire is to measure jitter, higher jitter values are desirable to overcome quantization limits; therefore, a larger separation would improve a jitter measurement system. Unfortunately there are limits to large separations because the source must be imaged in both apertures. A larger

separation limits the minimum distance sources can be imaged. Also note that having an aperture pair observing a source pair, the jitter is non-zero.

This experiment also demonstrates that a new imaging geometry is simply modeled with the path displacement σ which is dependent on the source and aperture geometries. And for each geometry there exists a weight vector.

```
# same code as before
# A single target target pair separated by 2 meters
target = [2.0/Atm.L, 0.0]
# A dual aperture is used with b[ii] separation (meters)
platform = [b[ii], 0.0]
# same code as before
```

Listing 3. Excerpt of code to generate jitter measurements for each platform altitude and platform separation values.

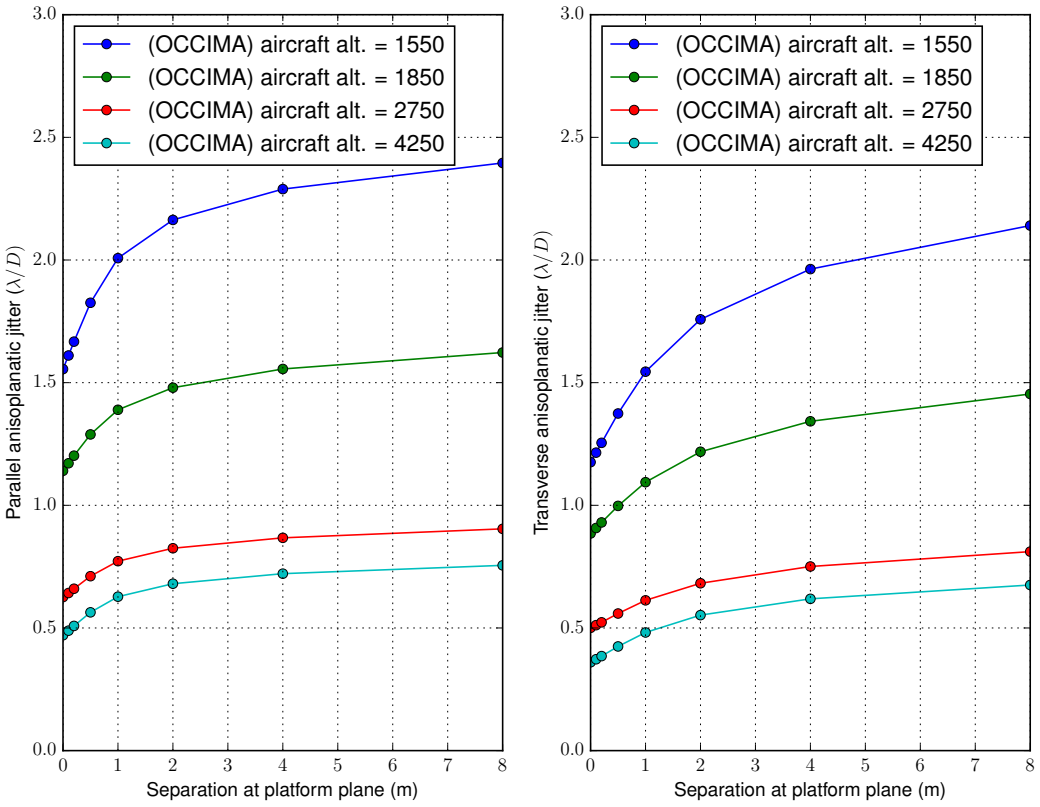

Figure 4. Experiment with jitter measurements from varying platform dual aperture separations and platform height values.

5. APPROACH TO C_N^2 ESTIMATION

To estimate C_n^2 along the imaging path, the approach taken by Whiteley [2] and that I take as well, is to discretize the path into slices as illustrated in Figure 5. Assume there are N partitions of equal size along the path length L, we may model turbulence strength partitions with

$$C_n^2(\xi L) = \sum_{i=1}^{N} C_{ni}^2 \,\text{rect}\left(\frac{\xi - \xi_i}{l_i}\right). \tag{27}$$

The normalized center of the ith partition is ξ_i and l_i is the normalized partition width. I assume that each slice is a good approximate of the C_n^2 in that local region. The vector $\mathbf{c} \in \mathbb{R}^N$ containing each i^{th} component of C_{ni}^2 is

$$\mathbf{c} = (C_{n1}^2, \ldots, C_{nN}^2)^T. \tag{28}$$

Let the jitter measurement vector $\mathbf{m} \in \mathbb{R}^K$ with K observations for each k^{th} component (in rad^2) be

$$m_k = \frac{\sigma_{uk}^2}{2^{13/3}\sqrt{3}\Gamma(8/3)D^{-1/3}L} = \langle \theta_u(\mathbf{r})\theta_u(\mathbf{r})\rangle - \langle \theta_u(\mathbf{r})\theta_u(\mathbf{r}_m)\rangle. \tag{29}$$

Using Equations (26), (27) and (29) the jitter measurement component is related to C_n^2 with

$$\mathbf{m} = \mathbf{P}\mathbf{c}, \tag{30}$$

where the scene geometry is encoded in the matrix $\mathbf{P} \in \mathbb{R}^{K\times N}$ with each row $\mathbf{p}_k \in \mathbb{R}^N$ having each component being an integration of the weight vectors,

$$p_{ki} = \int_{\xi_i - l_i/2}^{\xi_i + l_i/2} d\xi \left(W_{uu}(\xi;0) - W_{uu}(\xi;\sigma_k)\right), \tag{31}$$

where $W_{uu}(\xi;0)$ is the weighting along the path with $\sigma = 0 \,\forall\, \xi$. The subscripts u is to indicate either x or y direction relative to the separation axis and k to indicate which measurement geometry.

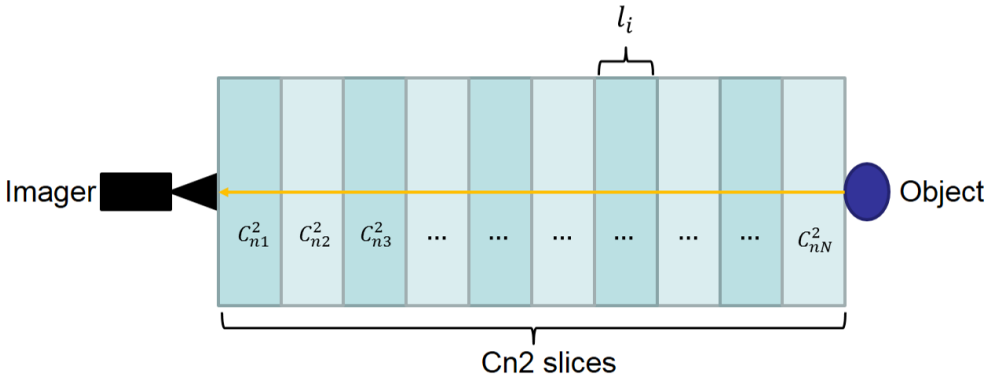

Figure 5. Illustration of arbitrary C_n^2 slices along an imaging path.

We now have a compact form with K observations with N turbulent partitions represented in linear form. A least-squares estimate of the vector $\mathbf{c}$ may be achieved with

$$\hat{\mathbf{c}} = \mathbf{P}^+\mathbf{m}, \tag{32}$$

$$\text{with pseudo-inverse } \mathbf{P}^+ = (\mathbf{P}^T\mathbf{P})^{-1}\mathbf{P}^T. \tag{33}$$

Whiteley refers to $\mathbf{P}^+$ as the "turbulence profile reconstructor". The jitters can then be compared for goodness of fit with $\hat{\mathbf{m}} = \mathbf{P}\hat{\mathbf{c}}$.

As an example of estimating $\mathbf{c}$, I have an experiment where there are multiple horizontal feature separations at the target plane between 0.01 to 2 meters. At the platform plane there are two imagers separated by a 0.5 meters. A random vector $\mathbf{c}$ was generated with $C_n^2 = C_0 * \exp(\sigma_t t)$ with $C_0 = 1 \times 10^{-14}$ and $t \sim N(0,1)$ and $\sigma_t = 2$. The jitter for this configuration is in Figure 6(a). The number of screens chosen for this experiment was eight screens. The true random vector $\mathbf{c}$ and estimated vector $\hat{\mathbf{c}}$ using Equation (32) is shown in Figure 6(b). The code to estimate the C_n^2 profile is deomonstrated in Listing 4.

```
# Measure parallel and transverse jitter,
# jitters_p and jitters_t, respectively
jitters = np.hstack((jitters_p, jitters_t))
# Precompute Wpp0, Wtt0, Wppm, Wttm
W['Wpp0'] = Wpp0
W['Wtt0'] = Wtt0
W['Wppm'] = Wppm
W['Wttm'] = Wttm
Cn2_est = Atm.estimateCn2_method_mza(W, jitters)
```

Listing 4. Excerpt of code to estimate $\mathbf{c}$ using OCCIMA python modules.

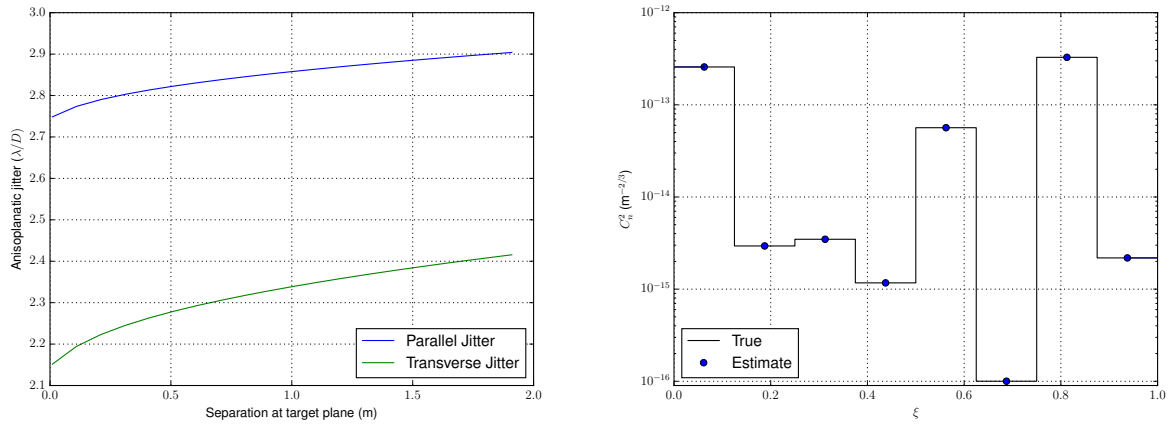

(a) (b)

Figure 6. Jitter and atmospheric profiling.

6. CONCLUSION

In this work I present the background to anisoplanatic jitter and how that relates to Zernike tilt covariance and ultimately the C_n^2 path profile. I then demonstrate OCCIMA code examples that match prior work from Magee, Das, and Welch [10] and I also show a new experiment using a dual imaging system instead of a single imager. Finally, I show how to estimate the C_n^2 profile given jitter measurements.

The method of estimating C_n^2 in a least-squares approach requires the matrix $\mathbf{P}$ to be well-conditioned. This matrix is only dependent on the scene geometry. In future work I will investigate methods of using joint multi-view imaging to improve the condition of the matrix $\mathbf{P}$, and hence improve accuracy of the estimate of $\mathbf{c}$. Likewise, I will investigate the eigen-decomposition of $\mathbf{P}$ to change the C_n^2 slice thickness from uniform to varying to optimize accuracy of estimation.

REFERENECES

1. Gibson, K. B. 2015. “Stereo Image Motion Monitor for Atmospheric Mitigation and Estimation.” SPIE Optical Engineering + Applications (pp. 961404–961404). International Society for Optics and Photonics.

2. Whiteley, M. R., D. C. Washburn, and L. A. Wright. 2002. “Differential-Tilt Technique for Saturation Resistant Profiling of Atmospheric Turbulence.” *International Symposium on Optical Science and Technology* (pp. 221–232). International Society for Optics and Photonics.

3. Kolmogorov, A. N. 1941. “The Local Structure of Turbulence in Incompressible Viscous Fluid for Very Large Reynolds Numbers.” Dokl. Akad. Nauk SSSR, vol. 30, pp. 299–303.

4. Fried, D. L. 1965. “Statistics of a Geometric Representation of Wavefront Distortion,” *Journal of the Optical Society of America*, vol. 55, no. 11, pp. 1427–1431.

5. Kallistratova, M., and A. Kon. 1966. “Fluctuations in the Angle of Arrival of Light Waves From an Extended Source in a Turbulent Atmosphere,” *Radiophysics and Quantum Electronics*, vol. 9, no. 6, pp.636–639.

6. Fried, D. L. 1975. “Differential Angle of Arrival: Theory, Evaluation, and Measurement Feasibility,” *Radio Scie*nce, vol. 10, no. 1, pp. 71–76.

7. Roggemann, M. C., B. M. Welsh, and B. R. Hunt. 1996. *Imaging Through Turbulence*. CRC Press. Boca Raton, FL.

8. Schmitt, J. D. 2010. *Numerical Simulation of Optical Wave Propagation With Examples in MATLAB.* SPIE Press Monograph Volume PM199. SPIE, Bellingham, WA.

9. Whiteley, M. R. 1998. “Optimal Atmospheric Compensation for Anisoplanatism in Adaptive-Optical Systems.” Doctoral thesis. Air Force Institute of Technology. Wright-Patterson Air Force Base Ohio.

10. Magee, E. P., M. R. Whiteley, S. T. Das, and B. M. Welsh. 2003. “Tilt Anisoplanatism in Extended Turbulence Propagation.” *Proceedings of SPIE 4976: High-Power Lasers and Applications* (pp. 13–21). International Society for Optics and Photonics.

REPORT DOCUMENTATION PAGE

Form Approved
OMB No. 0704-01-0188

1. REPORT DATE *(DD-MM-YYYY)*	2. REPORT TYPE	3. DATES COVERED *(From - To)*
September 2016	Final	

4. TITLE AND SUBTITLE

Preliminary Work in Atmospheric Turbulence Profiles with the Differential Multi-image Motion Monitor

5a. CONTRACT NUMBER

5b. GRANT NUMBER

5c. PROGRAM ELEMENT NUMBER

6. AUTHORS

Kristopher B. Gibson

5d. PROJECT NUMBER

5e. TASK NUMBER

5f. WORK UNIT NUMBER

7. PERFORMING ORGANIZATION NAME(S) AND ADDRESS(ES)

SSC Pacific
53560 Hull Street
San Diego, CA 92152–5001

8. PERFORMING ORGANIZATION REPORT NUMBER

TR 2053

9. SPONSORING/MONITORING AGENCY NAME(S) AND ADDRESS(ES)

SSC Pacific
Naval Innovative Science and Engineering (NISE) Program (Capability Investment)
53560 Hull Street
San Diego, CA 92152–5001

10. SPONSOR/MONITOR'S ACRONYM(S)

11. SPONSOR/MONITOR'S REPORT NUMBER(S)

12. DISTRIBUTION/AVAILABILITY STATEMENT

Approved for public release.

13. SUPPLEMENTARY NOTES

14. ABSTRACT

This report provides the background to anisoplanatic jitter and how that relates to Zernike tilt covariance and ultimately the C_n^2 path profile. Space and Naval Warfare Systems Center Pacific's (SSC Pacific) Optical Channel Characterization in Maritime Atmospheres (OCCIMA) Python code is demonstrated with examples that match prior work from past experiments with anisoplanatic jitter. A new experiment using a dual imaging system instead of a single imaging system is presented. And finally, this report demonstrates how to estimate the C_n^2 profile given jitter measurements.

15. SUBJECT TERMS

anisoplanatic jitter; Zernike tilt covariance; C_n^2 path profile estimation: dual imaging system; Optical Channel Characterization in Maritime Atmospheres (OCCIMA) code

16. SECURITY CLASSIFICATION OF:			17. LIMITATION OF ABSTRACT	18. NUMBER OF PAGES	19a. NAME OF RESPONSIBLE PERSON
a. REPORT	b. ABSTRACT	c. THIS PAGE			Kristopher B. Gibson
U	U	U	U	22	19B. TELEPHONE NUMBER *(Include area code)* (619) 553-4756

INITIAL DISTRIBUTION

84300	Library	(1)
85300	Archive/Stock	(1)
56430	K. B. Gibson	(1)

Defense Technical Information Center
Fort Belvoir, VA 22060–6218 (1)

Approved for public release.

SSC Pacific
San Diego, CA 92152-5001